Methionine Adenosyltransferase α-Helix Structure Unfolds at Lower Temperatures than β-Sheet: A 2D-IR Study

Ibon Iloro,* Rosana Chehín,* Félix M. Goñi,* María A. Pajares,† and José-Luis R. Arrondo*
*Unidad de Biofísica (Centro Mixto CSIC-UPV) and Departamento de Bioquímica, Universidad del País Vasco, Bilbao, Spain; and
†Instituto de Investigaciones Biomédicas "Alberto Sols" (CSIC-UAM), Madrid, Spain

ABSTRACT Two-dimensional infrared spectroscopy has been used to characterize rat liver methionine adenosyltransferase and the events taking place during its thermal unfolding. Secondary structure data have been obtained for the native recombinant enzyme by fitting the amide I band of infrared spectra. Thermal denaturation studies allow the identification of events associated with individual secondary-structure elements during temperature-induced unfolding. They are correlated to the changes observed in enzyme activity and intrinsic fluorescence. In all cases, thermal denaturation proved to be an irreversible process, with a T_m of 47–51°C. Thermal profiles and two-dimensional infrared spectroscopy show that unfolding starts with α-helical segments and turns, located in the outer part of the protein, whereas extended structure, associated with subunit contacts, unfolds at higher temperatures. The data indicate a good correlation between the denaturation profiles obtained from activity measurements, fluorescence spectroscopy, and the behavior of the infrared bands. A study of the sequence of events that takes place is discussed in light of the previous knowledge on methionine adenosyltransferase structure and oligomerization pathway.

INTRODUCTION

S-adenosylmethionine (AdoMet) is the main methyl donor for the transmethylation reactions carried out in the cell (Cantoni, 1975). The number of such reactions is as large as that of the processes in which ATP is involved (Mato et al., 1997). Synthesis of AdoMet is carried out by the enzyme named methionine adenosyltransferase (MAT) (EC 2.5.1.6) that has been detected even in the genome of *Mycoplasma genitalium*, considered to contain the minimum set of genes needed for independent life (Fraser et al., 1995). Two MAT isozymes have been identified in mammals; one is ubiquitous (MAT II), whereas the other is mainly expressed in the liver (Mato et al., 1997; Lu et al., 2003). The latter isoenzyme appears in two oligomeric assemblies, homotetramer (MAT I) and homodimer (MAT III), that differ in their affinity for methionine, one of its substrates (Alvarez et al., 1994; Cabrero et al., 1987). MAT I is 10-fold more active than MAT III at the physiological Met concentrations, a fact that has been proposed as an adaptive advantage for the clearance of high plasmatic levels of methionine. This function is carried out essentially by the liver, where 85% of the transmethylation reactions take place (Mudd and Poole, 1975; Cantoni, 1975). Under pathological conditions, such as liver cirrhosis, the ratio between MAT forms is altered (Cabrero et al., 1988). In fact, a decrease in MAT activity is detected that correlates with the presence of MAT III as the main liver isoform (Duce et al., 1988).

One MAT subunit consists of 396 amino acids (Alvarez et al., 1991; Horikawa et al., 1989) organized in three domains formed by nonconsecutive parts of the primary structure (Gonzalez et al., 2000). The N-terminal domain is formed by amino acids 17–28 and 146–254, the central domain by those at positions 29–116 and 255–289, and the C-terminal domain contains residues 129–145 and 290–396. Besides, the crystal structure allows the identification of a flexible loop connecting the central and C-terminal domains. The contact between subunits in the dimer is a large, flat hydrophobic surface, whereas the two dimers associate to form the tetramer through a few polar interactions. The subunit arrangement in the dimer is quite similar in the two structures known to date, *Escherichia coli* (Takusagawa et al., 1996) and rat liver (Gonzalez et al., 2000). However, the arrangement of dimers to form the tetramer differs slightly, including the number and type of contacts. Interactions between dimers in MAT I are established through the β-sheet where C35 and C61 (no equivalent to this residue exists in the *E. coli* enzyme) are located. As recently demonstrated, the generation of a disulfide bond between the -SH groups of these residues stabilizes the contact area, precluding dissociation processes (Sanchez-Perez et al., 2003). This could explain the presence of dimers in mammalian liver, whereas all other known MATs are either homo- or heterotetramers (Kotb and Geller, 1993; Mato et al., 1997).

The active sites, two per dimer, are located between subunits and constituted by amino acids from both (Gonzalez et al., 2000; Takusagawa et al., 1996). The folding pathway for MAT III involves one kinetic and one equilibrium intermediate (del Pino et al., 2002; Gasset et al., 2002). The equilibrium intermediate has been characterized as a monomer that binds less ANS (1-anilino-8-naphthalene sulfonate)

Submitted May 26, 2003, and accepted for publication February 3, 2004.

Address reprint requests to José-Luis R. Arrondo, Tel.: 34-946-012-485; Fax: 34-944-648-500; E-mail: gbproarj@lg.ehu.es.

Rosana Chehín's permanent address is INSIBIO, Universidad Nacional de Tucumán, Chacabuco 461, 4000 S.M. de Tucumán, Argentina.

0006-3495/04/06/3951/08 $2.00

doi: 10.1529/biophysj.103.028373

than the native dimer, and preserves ~70% of the native secondary structure. Oligomerization of MAT III to MAT I occurs when protein concentration is increased above a certain limit. Again association takes place through a kinetic intermediate that has also been identified (Sanchez-Perez et al., 2003).

Infrared (IR) spectroscopy has become a widely used tool in the study of protein structure (Tamm and Tatulian, 1997; Vigano et al., 2000; Barth, 2000; Barth and Zscherp, 2002). Structural analysis usually implies a mathematical approach to extract the information contained in the composite bands, designated in IR spectroscopy as ''amide bands'', arising from proteins. Commonly used methods of analysis involve narrowing the intrinsic bandwidths to visualize the overlapping band components and then decomposing the original band contour into these components by means of an iterative process. The various components are finally assigned to protein or subunit structural features (Arrondo and Goñi, 1999). External perturbations such as temperature are commonly used to obtain a deeper insight into protein structure by means of infrared spectroscopy. Thermal profiles have often been used to study conformational changes in proteins (Arrondo et al., 1994). Recently, the use of two-dimensional correlation spectroscopy (2D-IR) has been proposed. In this procedure the spectra before and after an external perturbation are correlated to increase the amount of information obtained from the infrared spectrum (Noda et al., 2000). Proteins are a good target for this method, since changes induced by temperature (Fabian et al., 1999), or by the presence of lipids (Shanmukh et al., 2002; Torrecillas et al., 2003) or other external ligands (Pastrana-Rios et al., 2002), can be studied in more detail than with the conventional infrared approach.

In the present work we have used conventional and 2D-IR to study the structure and thermal unfolding of MAT. Denaturation of the protein involves a loss of the subunit-subunit contacts and/or unfolding of the monomers leading to aggregation. Conventional infrared spectroscopy describes the thermal profile and the latter has been used as a guide to the regions to be analyzed using 2D-IR.

MATERIALS AND METHODS

Refolding and purification of recombinant rat liver MAT

Expression of rat liver MAT in *E. coli* and isolation of the inclusion bodies was carried out as previously described (Gonzalez et al., 2000; Lopez-Vara et al., 2000). The pellets were then washed as described and used for refolding in the presence of dithiothreitol using the two-step procedure. The refolded protein was purified on a Q-Sepharose column (2.5 × 18 cm) (Pharmacia LKB, Sweden) and the active fractions collected after measuring MAT activity. The peak was pooled and concentrated by ultrafiltration using YM-30 membranes (Amicon Corp., Beverly, MA). The concentrate (4 ml) was then loaded on a Biogel A gel filtration column (1.5 × 95 cm) (Bio-Rad, Richmond, CA) and eluted in 10 mM Hepes/Na, pH 7.5, 10 mM $MgSO_4$, and 50 mM KCl. Fractions were tested for activity, the peak pooled and dialyzed to reduce the presence of KCl before Amicon concentration to reach 10 mg/ml, as determined using the Bio-Rad protein assay kit and bovine serum albumin as the standard. MAT purity was assessed by sodium dodecyl sulfate polyacrylamide gel electrophoresis (Laemmli, 1970).

Determination of methionine adenosyltransferase activity

MAT activity was measured essentially as described previously (Gil et al., 1997), using protein concentrations of 0.05 mg/ml. Protein samples were incubated for 5 min at temperatures between 20 and 75°C before activity was measured. To test for reversibility, a sample of the heat-inactivated proteins was incubated in a 20°C bath for 5 min before MAT activity determination.

Intrinsic fluorescence experiments

Samples at 0.05 mg/ml were excited at 295 nm; the slit width was 2.5 nm for excitation and 5 nm for emission. Fluorescence intensities were recorded at the maximum of the emission band between 300 and 400 nm in a SLM-8000 spectrofluorometer, using 0.5 × 0.5 cm cuvettes. The fluorescence signal for the protein was corrected by subtraction of the solvent signal.

Infrared studies

The protein samples were measured typically at 10 mg/ml in 10 mM Hepes, pH 7.5. The spectra were recorded in a Nicolet Magna II 550 spectrometer equipped with a mercury-cadmium-telluride detector using a demountable liquid cell (Harrick Scientific, Ossining, NY) with calcium fluoride windows, using 6-μm spacers in the H_2O medium and 50-μm spacers in the D_2O measurements. A tungsten-copper thermocouple was placed directly onto the window and the cell placed into a thermostated cell mount. Typically 1000 scans for each, background and sample, were collected and the spectra obtained with a nominal resolution of 2 cm^{-1}. Data treatment and band decomposition of the original amide I have been described elsewhere (Arrondo et al., 1993; Arrondo and Goñi, 1999; Bañuelos et al., 1995). The mathematical solution to the decomposition may not be unique, but if restrictions are imposed such as the maintenance of the initial band positions in an interval of $\approx$1 cm^{-1}, the preservation of the bandwidth within the expected limits, or the agreement with theoretical boundaries or predictions, the result becomes, in practice, unique.

Thermal analysis was performed in the 30–80°C interval in 3° steps. At every step, the sample was left to equilibrate and the spectra measured as described above. To obtain the 2D-IR maps, heating was used as the perturbation to induce time-dependent spectral fluctuations and to detect dynamic spectral variations on the secondary structure of MAT. Obtention of the two-dimensional synchronous and asynchronous spectra has been described previously (Turnay et al., 2002).

RESULTS

Native state of methionine adenosyltransferase

The infrared amide I band, located between 1700 and 1600 cm^{-1} and arising mainly from the C=O stretching vibration of the peptide bond, is conformationally sensitive and can be used to monitor either the secondary structure composition or the changes induced in the protein structure by external agents such as temperature. Differences in dihedral angles and/or hydrogen-bonding patterns among the different protein conformations give rise to a composite band enclosing the structural information of the protein (Arrondo

and Goñi, 1999). The information can be extracted using different mathematical techniques. Band-narrowing procedures allow the determination of the number and position of the components, although those techniques do not produce an increment in resolution, and the treated spectra cannot be used to quantify the protein structure. Fig. 1 shows the amide I region of MAT IR spectra in H_2O and D_2O media together with the band components and the fitted spectra. The band components, area percentages, and assignments are shown in Table 1. The structure of the tetramer (MAT I) has been solved (Gonzalez et al., 2000), and it is known to be an α/β protein. The infrared spectrum is dominated both in H_2O and D_2O by two prominent bands at $\sim$1652 cm^{-1} and 1636 cm^{-1} attributed to α-helix and β-sheet, respectively. Bands at frequencies $<$1630 cm^{-1} were first described for extended polylysine chains (Susi, 1969) and attributed to antiparallel-chain pleated sheet with intermolecular hydrogen bonding. More recently (Kubelka and Keiderling, 2001) a shift in band position at $<$1630 cm^{-1} has also been described in peptides as produced by multiple-stranded structures. Bands $<$1630 cm^{-1} were also found in denatured proteins in D_2O buffer (Arrondo et al., 1994; Van Stokkum et al., 1995) that could not, after aggregation, revert to the original conformation. However, they are not common in native proteins either in H_2O or in D_2O. In native proteins, a band at a wavenumber lower than 1630 cm^{-1} was first found in concanavalin A (Arrondo et al., 1988) and assigned to proteins in an extended configuration, with a hydrogen-bonding pattern formed by peptide residues not taking part in intramolecular β-sheet, but rather hydrogen-bonded to other molecular structures, e.g., forming intermolecular hydrogen bonding in monomer-monomer interaction (Barth and Zscherp, 2002). The presence of these low-frequency bands in nondenatured proteins has been found in other proteins establishing contacts through α-helices such as tyrosine hydroxylase (Martínez et al., 1996), known to be tetrameric from x-ray diffraction (Goodwill et al., 1997). Thus the band observed at 1624 cm^{-1} in the MAT spectrum in D_2O, and at 1626 cm^{-1} in H_2O, would agree with its existence as an oligomeric protein, as expected from the concentration range used in our studies (Sanchez-Perez et al., 2003). On the basis of these assignments (Table 1), it is possible to calculate the secondary structure composition of the sample which would be of $\sim$4% α-helix, 37% β-sheet, and 18% β-turns. It must be noted that no band around 1643 cm^{-1} is present in D_2O medium and that the percentage of the 1652 cm^{-1} band in H_2O and D_2O is very similar.· Hence it can be concluded that the amount of unordered structure, as defined by the infrared spectra, is low in this protein.

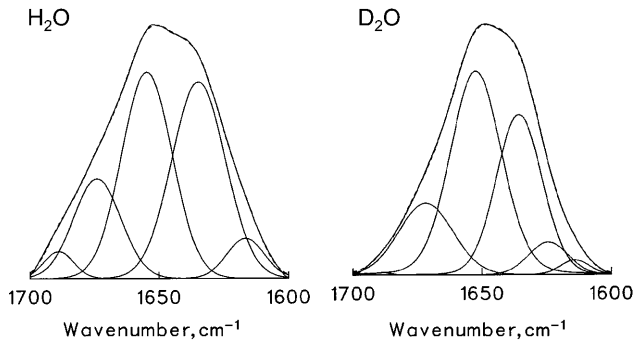

FIGURE 1 Amide I band decomposition of MAT in H_2O (*left*) or in D_2O (*right*) media. The dashed line corresponds to the sum of the band components. The numerical values are presented in Table 1.

Methionine adenosyltransferase thermal profile

The study of protein structural changes caused by an external perturbation such as temperature provides information on the conformation and organization of the protein during unfolding. Fig. 2 shows a plot of the MAT-deconvolved amide I band in D_2O in the 20–80°C interval. At high temperatures, the infrared spectrum is characterized by the appearance of two bands around 1618 and 1685 cm^{-1}, representative of protein aggregation. Temperature-dependent denaturation of MAT is not reversible as judged from the results obtained by either activity measurements or fluorescence and infrared spectroscopies (not shown). The change in bandshape seen upon protein denaturation can be correlated with loss of enzyme activity and changes in the protein intrinsic fluorescence (Fig. 3). Moreover, amide I band decomposition allows the temperature-dependent study of specific spectral changes such as the appearance of the aggregation band, or variations in the bands corresponding to α-helix (Fig. 3 *A*). The parameters in Fig. 3 define three regions: region I, of full enzyme activity (20–37°C); region II, of activity loss with concomitant changes in the fluorescence and infrared spectra (37–55°C); and region III ($>$55°C), in which activity is zero and no further changes in intrinsic fluorescence or infrared bands are detected. T_m for the loss of activity is 51°C, and the corresponding value for the decrease in intrinsic fluorescence is 50°C. From the infrared profile monitored by the shift in the 1624 cm^{-1} band (Fig. 3), concomitant with changes in the amide I bandwidth (not shown), the midpoint of the denaturation process is estimated at 47°C. Representative spectra from each region are shown in Fig. 4, and the corresponding parameters are summarized in Table 2. Note that the β-sheet percentage (1635 cm^{-1} band) does not vary substantially with temperature. In turn, the 1652 cm^{-1} band attributed to α-helix splits upon heating into two components at 1649 and 1661 cm^{-1}.

However, the sequence of changes and interactions induced by temperature on the protein cannot be deduced from these thermal profiles and curve-fittings. Hence, additional analysis is needed to monitor in detail the temperature-induced changes. 2D-IR correlation spectroscopy can detect small variations in the spectra, and also the interband interactions accounting for these changes. In

TABLE 1 Band position, % area, and assignment of the components obtained after curve-fitting of MAT infrared spectra in H_2O and D_2O media at 25°C

H_2O			D_2O		
Band position (cm^{-1})	Assignment	% Area	Band position (cm^{-1})	Assignment	% Area
1689	High frequency β-sheet	3	1690	β-turns	<1
1674	β-turns	18	1672	β-turns + high frequency β-sheet	18
1654	α-helix	44	1652	α-helix	44
1636	β-sheet	25	1635	β-sheet	28
1626	Extended β-interoligomer interactions	10	1624	Extended β-interoligomer interactions	9

The values have been rounded off to the nearest integer.

a synchronous 2D map, the peaks located along the diagonal (autopeaks) correspond to changes in intensity induced (in this case) by temperature and they are always positive. The cross-relation peaks indicate an in-phase relationship between the two bands involved, i.e., that two vibrations of the protein, characterized by two different wavenumbers (ν_1 and ν_2), are being affected simultaneously. Asynchronous maps show not-in-phase cross-relation between the bands and give an idea of the sequential order of events produced by the perturbation, i.e., an asynchronous peak is produced if the vibrations of the functional groups corresponding to the varying wavenumbers change each at a different time. The asynchronous peak will be positive if the change in ν_1 occurs earlier than that in ν_2, and negative in the opposite case. To study the different events taking place during the thermal unfolding of MAT, correlation maps corresponding to the three regions indicated by the thermal profiles of activity, infrared, and fluorescence spectra have been studied.

Events in region I

The 2D synchronous (*left*) and asynchronous (*right*) maps corresponding to region I are depicted in Fig. 5. The synchronous plot shows autopeaks at 1622, 1652, 1668, and 1682 cm^{-1}, indicating temperature-dependent intensity changes in these peaks. Note that no autopeak corresponding to the 1635 cm^{-1} band (β-sheet) is present, whereas the α-helix band is clearly seen. Positive cross-correlation peaks in this region, indicating that both peaks either increase or decrease in intensity, are found for the band pairs 1622/1644, 1622/1662, 1622/1682, and 1662/1682 cm^{-1}. The negative band pairs are 1622/1652, 1652/1662, and 1652/1680 cm^{-1}, indicating that these peak intensities follow an opposite behavior, i.e., one increases whereas the other decreases. Asynchronous maps are symmetrical; the asynchronous plot

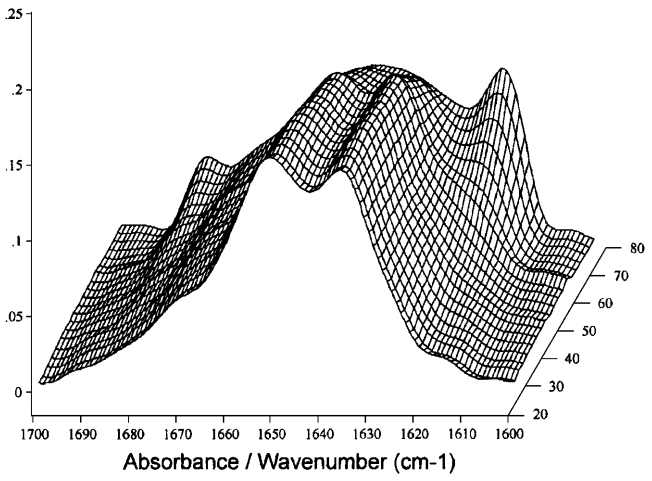

FIGURE 2 Temperature plot of the deconvolved amide I region in D_2O buffer in the 20–80°C interval showing the appearance of the aggregation bands at 1617 and 1685 cm^{-1}.

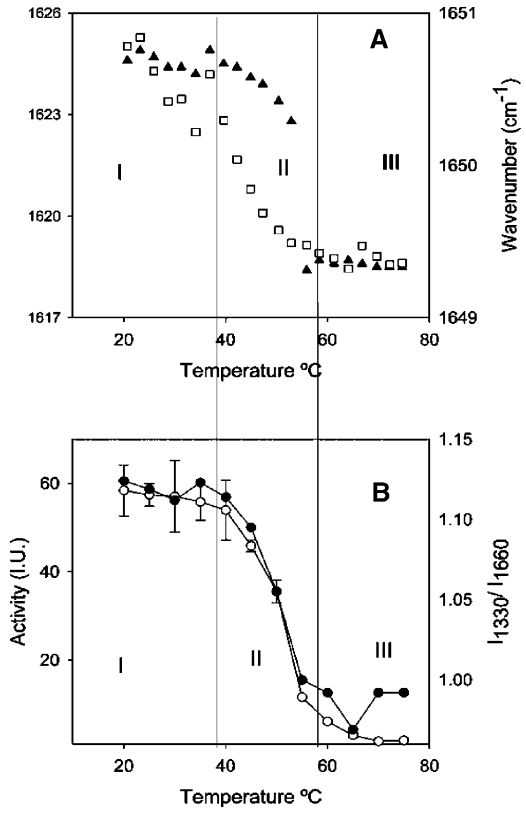

FIGURE 3 Thermal profile of MAT. (*A*) Traces corresponding to the IR 1652 cm^{-1} band (□) assigned to α-helix and 1624 cm^{-1} band (▲) corresponding to the oligomer interactions in MAT measured in D_2O buffer. (*B*) Profiles corresponding to protein activity (●) and intrinsic fluorescence (○).

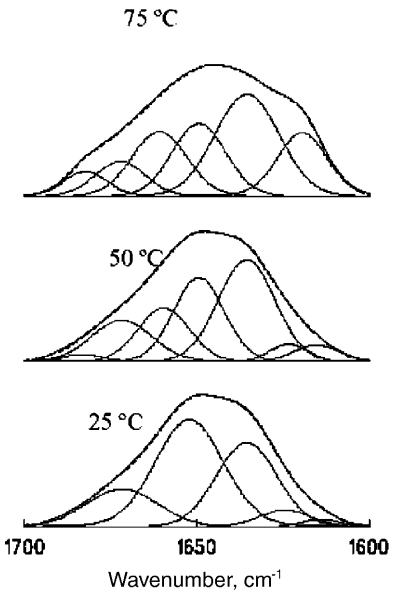

FIGURE 4 Amide I band decomposition corresponding to MAT in region I at 25°C (*bottom*), at 50°C in region II (*middle*), and at 75°C in region III (*top*). The spectra are measured in D_2O medium.

corresponding to this region shows correlation peaks corresponding to the pairs 1621/1645, 1621/1662, and 1621/1675 cm^{-1}. The three pairs are negative and their intensity is similar, indicating that they are the earliest events taking place during protein unfolding and that the change taking place at the second wavenumber of each pair occurs earlier than the one occurring at the first wavenumber. Therefore, the change of the bands at 1645, 1662, and 1675 cm^{-1} would be the first event in MAT thermal unfolding, indicating the loss of the oligomer interaction band at 1624 cm^{-1} and the rise in the 1617 cm^{-1} aggregation band. These results would confirm the low-temperature start of the 1624 cm^{-1} band change (Fig. 3).

Events in region II

In the infrared thermal profiles shown in Fig. 3, the various amide I band components display different behaviors in this region. The oligomerization band originally at ~1624 cm^{-1} follows a pattern similar to the change in activity, and the same is true of the α-helix band. Note, however, that the thermal shift in band position of the α-helix component occurs at ~10°C above that of the oligomer band component. Region II also comprises major changes in activity and intrinsic fluorescence.

TABLE 2 Parameters obtained after amide I band decomposition of MAT in D_2O buffer at 25°C, 50°C, and 75°C, corresponding to regions I, II, and III, respectively, of the thermal denaturation profile

25°C		50°C		75°C	
Band position	% Area	Band position	% Area	Band position	% Area
1690	<1	1693	<1		
		1686	3	1682	5
1672	18	1672	17	1672	9
		1660	19	1661	18
1652	44	1650	26	1649	19
1635	29	1636	31	1635	33
1624	8	1624	4	1618	16

The correlation maps corresponding to region II are shown in Fig. 6. The synchronous plot shows autopeaks at 1617, 1635, and 1652 cm^{-1}. Positive crosspeaks are located at 1617/1682 and 1635/1652 cm^{-1}. Negative ones are at 1617/1635 and 1617/1652 cm^{-1}, indicating that now both structures, α-helix and β-sheet, are affected by aggregation/denaturation. The asynchronous map shows the main correlation peaks at 1617/1635 and 1617/1652 cm^{-1}, indicating again that the major event taking place in region II is the rise of the 1617 cm^{-1} aggregation band, simultaneous with changes in the α and β components.

Events in region III

Region III comprises the highest temperature range, once denaturation has taken place. Correlation maps (Fig. 7) are less complex since no further major changes in protein conformation are taking place. The synchronous map shows an autopeak at 1617 cm^{-1}, negative cross-correlation peaks at 1617/1635 and 1617/1652 cm^{-1}, and a faint positive crosspeak at 1617/1682 cm^{-1}. The asynchronous spectrum does not show peaks above the noise level, a typical behavior when only changes in intensity without bandshifts or variations in bandwidth are produced (Paquet et al., 2001; Arrondo et al., 2004).

DISCUSSION

The process of MAT thermal unfolding and aggregation has been divided into three regions according to the activity, intrinsic fluorescence, and infrared-amide I spectral characteristics. For this purpose, the native secondary structure composition calculated from the infrared spectra was first established (Table 1). Comparison of the percentage secondary structure data from infrared (this paper) and circular dichroism (Lopez-Vara et al., 2000) shows similar contents of β-sheet (37% and 34%, respectively) and turns (18% and 20%, respectively). However, circular dichroism detects 27% random coil, whereas IR detects no unordered structure in this protein (see below). X-ray diffraction data (González et al., 2000) indicate 23% α-helix and 19% β-sheet, but more than half the protein secondary structure is not assigned in the x-ray study. Whereas in CD some loops are assimilated to unordered structure, in IR spectra a loop has usually a defined assignment (Barth and Zscherp, 2002) and, opposite to unordered structure, it does not shift by >10 cm^{-1} from H_2O to D_2O. Moreover, unordered structure broadens the amide I bandshape in D_2O medium (Echabe

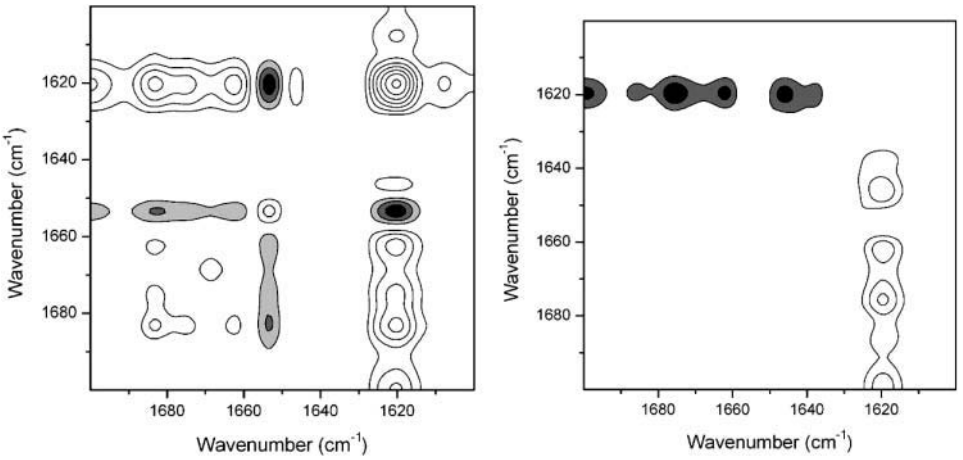

FIGURE 5 Synchronous (*left*) and asynchronous (*right*) correlation map contour in the 1700–1600 cm^{-1} interval of MAT IR spectra in the 25–37°C range, in which full enzyme activity is maintained. White peaks correspond to positive correlations and gray peaks to negative ones.

et al., 1998). However, in Fig. 1 the bandshape is very similar in both media, pointing to a low content of unordered structure in MAT. The data for the native protein calculated by these techniques is important to assign the thermal changes, and for future comparisons with mutants.

Region I would correspond to a functional tetrameric protein without changes in the 20–34°C range, the unfolding beginning at 37°C, as determined by the classical infrared approach. The 2D-IR correlational maps (Fig. 5) allow the study of the less apparent processes taking place during protein unfolding. In both the synchronous and asynchronous maps of spectra in the 20–37°C interval, the dominant peak is centered at ~1622 cm^{-1} and corresponds to the peak originally at 1624 cm^{-1} that shifts to 1617 cm^{-1} after denaturation. This shift corresponds to changes in protein contacts and marks the beginning of aggregation, as seen in Fig. 2. The 1622 cm^{-1} band is correlated in the synchronous spectrum with peaks corresponding to α-helix, unordered structure, and β-turns, but not with the one corresponding to β-sheet. In the asynchronous spectrum similar cross-correlations are observed, excluding the β-sheet. Also, in the asynchronous spectrum, cross-correlations of the 1622 cm^{-1} peak with α-helix and β-turns are the most intense ones, indicating that these structures are the first to be perturbed by temperature. Thus, considering the x-ray MAT structure (Gonzalez et al., 2000) and the assignments stated above, the sequence of events that would take place in the protein would be 1), an unfolding of the outer part of the monomers composed mainly of α-helix and turns, together with 2), exposure of hydrophobic residues, followed by 3), establishment of intermolecular hydrogen bonds (Ismail et al., 1992; Muga et al., 1991). Changes in a band at ~1624 cm^{-1} have also been observed and assigned to a monomerization process in the unfolding of sarcoplasmic reticulum Ca^{2+}-ATPase (Echabe et al., 1998). Judging from the infrared and structural data it is not possible to conclude unequivocally in the present case whether the process is a tetramer-dimer-monomer or a direct tetramer-monomer transition.

In region II, a more simple pattern appears to take place. Here activity is being gradually lost and changes in fluorescence intensity are detectable at protein concentrations at which the dimer should prevail (Sanchez-Perez et al., 2003). Both infrared maps (Fig. 6) show that aggregation is

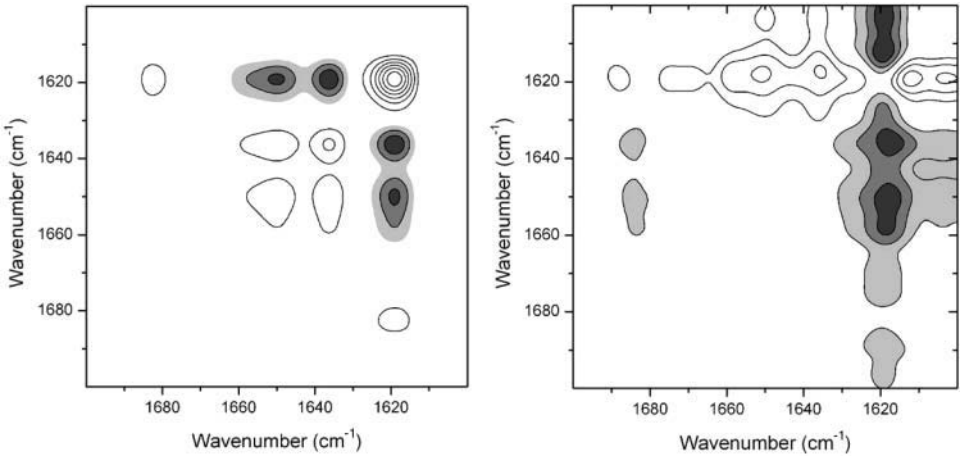

FIGURE 6 Synchronous (*left*) and asynchronous (*right*) correlation map contour in the region 1700–1600 cm^{-1} of MAT in the interval 37–53°C, in which enzyme activity is being lost. White peaks correspond to positive correlations and gray peaks to negative ones.

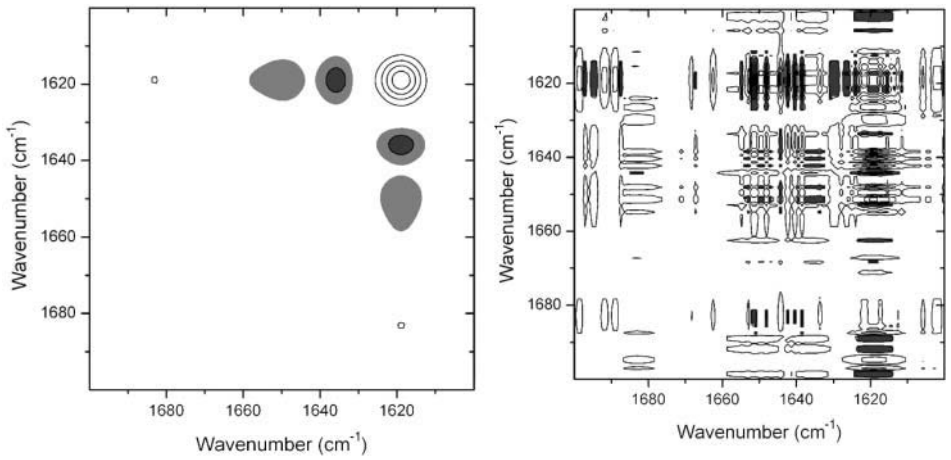

FIGURE 7 Synchronous (*left*) and asynchronous (*right*) correlation map contour in the region 1700–1600 cm^{-1} of MAT in the interval 53–80°C, after enzyme activity has been lost. White peaks correspond to positive correlations and gray peaks to negative ones.

happening at the expense of α-helix and β-sheet, and also of the residual β-turns. The small increase in area observed in the band fitting at 75°C for the 1635 cm^{-1} component (Table 2) would point to other concomitant interconversions. Note in the synchronous spectrum the pattern formed by the autopeaks at 1652 and 1635 cm^{-1}, the cross-correlations between them, and the faint intensity in the middle. This pattern is observed in simulations made with two bands simultaneously changing their intensities, either increasing or decreasing (Arrondo et al., 2004), indicating that in this region both α-helix and β-sheet change simultaneously, presumably decreasing in intensity. The fact that simulation patterns can be found in real proteins opens an interesting field to expand the potential of the 2D-IR analysis. As for MAT, inactivation and aggregation can be ascribed both to dimer dissociation and aggregation of the monomers, or just to aggregation of unfolded dimers. These phenomena cannot be distinguished with the techniques used in this study.

After losing activity once complete aggregation has been reached, the 2D-IR asynchronous correlation map (Fig. 7) shows only noise, because only changes in intensity occur (Paquet et al., 2001). The synchronous map is simple and shows the increase in aggregation. In this region no further unfolding takes place, but this does not imply that all the protein is aggregated, since some residual secondary structure can be present in inactive, aggregated proteins (Arrondo and Goñi, 1999). Note that when the protein is fully active and no variations in the amide I band are detected (20–34°C), the synchronous map (data not shown) consists only of noise, the same being true for the asynchronous map when only intensity changes take place.

In summary, 2D-IR is a useful method to characterize the thermal unfolding of an oligomeric protein, providing a deeper insight than the conventional infrared approach. MAT thermal unfolding is shown to be a process characterized by a series of steps starting at the structures located preferentially in the hydrophilic surfaces of the tetramer, that is, helices and turns. This step is followed by loss of the tetramer structure, to render probably a dimer still active within a narrow range of temperatures, and later by the unfolding and aggregation of the remaining protein structures. Also, the cross-correlation peaks in the 2D maps demonstrate that some protein structural components can interconvert during the unfolding process, e.g., helices to turns, turns to unordered, etc. Structural interconversions in protein denaturation are a novel feature that deserves further investigation.

The authors thank F. Garrido for technical assistance.

This work was supported by grant BMC2002-01438 (Ministerio de Ciencia y Tecnología) and 9/UPV00042.310-13552 from Universidad del Pais Vasco. M.A.P. was supported by grant 01/1077 (Fondo de Investigación Sanitaria), grant BMC2002-00243 (Ministerio de Ciencia y Tecnología), and Red de Centros RCMN (C03/08).

REFERENCES

Alvarez, L., M. Asuncion, F. Corrales, M. A. Pajares, and J. M. Mato. 1991. Analysis of the 5′ noncoding region of rat-liver S-adenosylmethionine synthetase messenger-RNA and comparison of the Mr deduced from the cDNA sequence and the purified enzyme. *FEBS Lett.* 290: 142–146.

Alvarez, L., J. Mingorance, M. A. Pajares, and J. M. Mato. 1994. Expression of rat liver S-adenosylmethionine synthetase in *Escherichia coli* results in two active oligomeric forms. *Biochem. J.* 301:557–561.

Arrondo, J. L. R., J. Castresana, J. M. Valpuesta, and F. M. Goñi. 1994. The structure and thermal denaturation of crystalline and non-crystalline cytochrome oxidase as studied by infrared spectroscopy. *Biochemistry.* 33:11650–11655.

Arrondo, J. L. R., and F. M. Goñi. 1999. Structure and dynamics of membrane proteins as studied by infrared spectroscopy. *Prog. Biophys. Mol. Biol.* 72:367–405.

Arrondo, J. L. R., I. Iloro, J. Aguirre, and F. M. Goñi. 2004. A two-dimensional IR spectroscopic (2D-IR) simulation of protein conformational changes. *Spectroscopy.* 18:49–58.

Arrondo, J. L. R., A. Muga, J. Castresana, and F. M. Goñi. 1993. Quantitative studies of the structure of proteins in solution by Fourier-transform infrared spectroscopy. *Prog. Biophys. Mol. Biol.* 59:23–56.

Arrondo, J. L. R., N. M. Young, and H. H. Mantsch. 1988. The solution structure of concanavalin A probed by FT-IR spectroscopy. *Biochim. Biophys. Acta.* 952:261–268.

Bañuelos, S., J. L. R. Arrondo, F. M. Goñi, and G. Pifat. 1995. Surface-core relationships in human low density lipoprotein as studied by infrared spectroscopy. *J. Biol. Chem.* 270:9192–9196.

Barth, A. 2000. The infrared absorption of amino acid side chains. *Prog. Biophys. Mol. Biol.* 74:141–173.

Barth, A., and C. Zscherp. 2002. What vibrations tell us about proteins. *Q. Rev. Biophys.* 35:369–430.

Cabrero, C., A. M. Duce, P. Ortiz, S. Alemany, and J. M. Mato. 1988. Specific loss of the high-molecular-weight form of S-adenosyl-L-methionine synthetase in human liver cirrhosis. *Hepatology.* 8:1530–1534.

Cabrero, C., J. Puerta, and S. Alemany. 1987. Purification and comparison of two forms of S-adenosyl-L-methionine synthetase from rat liver. *Eur. J. Biochem.* 170:299–304.

Cantoni, G. L. 1975. Biological methylation: selected aspects. *Annu. Rev. Biochem.* 44:435–451.

del Pino, M. M. S., I. Perez-Mato, J. M. Sanz, J. M. Mato, and F. J. Corrales. 2002. Folding of dimeric methionine adenosyltransferase III: identification of two folding intermediates. *J. Biol. Chem.* 277:12061–12066.

Duce, A. M., P. Ortiz, C. Cabrero, and J. M. Mato. 1988. S-adenosyl-L-methionine synthetase and phospholipid methyltransferase are inhibited in human cirrhosis. *Hepatology.* 8:65–68.

Echabe, I., U. Dornberger, A. Prado, F. M. Goñi, and J. L. R. Arrondo. 1998. Topology of sarcoplasmic reticulum Ca^{2+}-ATPase: an infrared study of thermal denaturation and limited proteolysis. *Protein Sci.* 7:1172–1179.

Fabian, H., H. H. Mantsch, and C. P. Schultz. 1999. Two-dimensional IR correlation spectroscopy: sequential events in the unfolding process of the lambda Cro-V55C repressor protein. *Proc. Natl. Acad. Sci. USA.* 96:13153–13158.

Fraser, C. M., J. D. Cocayne, O. White, M. D. Adams, R. A. Clayton, R. D. Fleischmann, C. J. Bult, A. R. Kerlavage, G. Sutton, J. M. Kelley, J. L. Fritchman, J. F. Weidman, K. V. Small, M. Sandusky, J. Fuhrmann, D. Nguyen, T. R. Utterback, D. M. Saudek, C. A. Phillips, J. M. Merrick, J. F. Tomb, B. A. Dougherty, K. F. Bott, P. C. Hu, T. S. Lucier, S. N. Peterson, H. O. Smith, C. A. Hutchison, and J. C. Venter. 1995. The minimal gene complement of Mycoplasma genitalium. *Science.* 270: 397–403.

Gasset, M., C. Alfonso, J. L. Neira, G. Rivas, and M. A. Pajares. 2002. Equilibrium unfolding studies of the rat liver methionine adenosyltransferase III, a dimeric enzyme with intersubunit active sites. *Biochem. J.* 361:307–315.

Gil, B., M. A. Pajares, J. M. Mato, and L. Alvarez. 1997. Glucocorticoid regulation of hepatic S-adenosylmethionine synthetase gene expression. *Endocrinology.* 138:1251–1258.

González, B., M. A. Pajares, J. A. Hermoso, L. Alvarez, F. Garrido, J. R. Sufrin, and J. Sanz-Aparicio. 2000. The crystal structure of tetrameric methionine adenosyltransferase from rat liver reveals the methionine-binding site. *J. Mol. Biol.* 300:363–375.

Goodwill, K. E., C. Sabatier, C. Marks, R. Raag, P. F. Fitzpatrick, and R. C. Stevens. 1997. Crystal structure of tyrosine hydroxylase at 2.3 Å and its implications for inherited neurodegenerative diseases. *Nat. Struct. Biol.* 4:578–585.

Horikawa, S., M. Ishikawa, H. Ozasa, and K. Tsukada. 1989. Isolation of a cDNA encoding the rat-liver S-adenosylmethionine synthetase. *Eur. J. Biochem.* 184:497–501.

Ismail, A. A., H. H. Mantsch, and P. T. T. Wong. 1992. Aggregation of chymotrypsinogen: portrait by infrared spectroscopy. *Biochim. Biophys. Acta.* 1121:183–188.

Kotb, M., and A. M. Geller. 1993. Methionine adenosyltransferase: structure and function. *Pharmacol. Ther.* 59:125–143.

Kubelka, J., and T. A. Keiderling. 2001. The anomalous infrared amide I intensity distribution in ^{13}C isotopically labeled peptide-sheets comes from extended, multiple-stranded structures. An ab initio study. *J. Am. Chem. Soc.* 123:6142–6150.

Laemmli, U. K. 1970. Cleavage of structural proteins during the assembly of the head of bacteriophage T_4. *Nature.* 193:680–685.

Lopez-Vara, M. C., M. Gasset, and M. A. Pajares. 2000. Refolding and characterization of rat liver methionine adenosyltransferase from Escherichia coli inclusion bodies. *Protein Expr. Purif.* 19:219–226.

Lu, S. C., I. Gukovsky, A. Lugea, C. N. Reyes, Z. Z. Huang, L. Chen, J. M. Mato, T. Bottiglieri, and S. J. Pandol. 2003. Role of S-adenosylmethionine in two experimental models of pancreatitis. *FASEB J.* 17:56–58.

Martínez, A., J. Haavik, T. Flatmark, J. L. R. Arrondo, and A. Muga. 1996. Conformational properties and stability of tyrosine hydroxylase studied by infrared spectroscopy. Effect of iron/catecholamine binding and phosphorylation. *J. Biol. Chem.* 271:19737–19742.

Mato, J. M., L. Alvarez, P. Ortiz, and M. A. Pajares. 1997. S-adenosylmethionine synthesis: molecular mechanisms and clinical implications. *Pharmacol. Ther.* 73:265–280.

Mudd, S. H., and J. R. Poole. 1975. Labile methyl balances for normal humans on various dietary regimens. *Metabolism.* 24:721–735.

Muga, A., H. H. Mantsch, and W. K. Surewicz. 1991. Apocytochrome c interaction with phospholipid membranes studied by Fourier-transform infrared spectroscopy. *Biochemistry.* 30:2629–2635.

Noda, I., A. E. Dowrey, C. Marcott, G. M. Story, and Y. Ozaki. 2000. Generalized two-dimensional correlation spectroscopy. *Appl. Spectrosc.* 54:236A–248A.

Paquet, M. J., M. Laviolette, M. Pezolet, and M. Auger. 2001. Two-dimensional infrared correlation spectroscopy study of the aggregation of cytochrome c in the presence of dimyristoylphosphatidylglycerol. *Biophys. J.* 81:305–312.

Pastrana-Rios, B., W. Ocana, M. Rios, G. L. Vargas, G. Ysa, G. Poynter, J. Tapia, and J. L. Salisbury. 2002. Centrin: its secondary structure in the presence and absence of cations. *Biochemistry.* 41:6911–6919.

Sanchez-Perez, G. F., M. Gasset, J. J. Calvete, and M. A. Pajares. 2003. Role of an intrasubunit disulfide in the association state of the cytosolic homo-oligomer methionine adenosyltransferase. *J. Biol. Chem.* 278: 7285–7293.

Shanmukh, S., P. Howell, J. E. Baatz, and R. A. Dluhy. 2002. Effect of hydrophobic surfactant proteins SP-B and SP-C on phospholipid monolayers. Protein structure studied using 2D IR and beta correlation analysis. *Biophys. J.* 83:2126–2141.

Susi, H. 1969. Infrared spectra of biological macromolecules and related systems. *In* Structure and Stability of Biological Macromolecules. S. N. Timasheff and L. Stevens, editors. Marcel Dekker, New York. 575–663.

Takusagawa, F., S. Kamitori, S. Misaki, and G. D. Markham. 1996. Crystal structure of S-adenosylmethionine synthetase. *J. Biol. Chem.* 271: 136–147.

Tamm, L. K., and S. A. Tatulian. 1997. Infrared spectroscopy of proteins and peptides in lipid bilayers. *Q. Rev. Biophys.* 30:365–429.

Torrecillas, A., S. Corbalan-Garcia, and J. C. Gomez-Fernandez. 2003. Structural study of the C2 domains of the classical PKC isoenzymes using infrared spectroscopy and two-dimensional infrared correlation spectroscopy. *Biochemistry.* 42:11669–11681.

Turnay, J., N. Olmo, M. Gasset, I. Iloro, J. L. R. Arrondo, and M. A. Lizarbe. 2002. Calcium-dependent conformational rearrangements and protein stability in chicken annexin A5. *Biophys. J.* 83:2280–2291.

Van Stokkum, I. H. M., H. Linsdell, J. M. Hadden, P. I. Haris, D. Chapman, and M. Bloemendal. 1995. Temperature-induced changes in protein structures studied by Fourier transform infrared spectroscopy and global analysis. *Biochemistry.* 34:10508–10518.

Vigano, C., L. Manciu, F. Buyse, E. Goormaghtigh, and J. M. Ruysschaert. 2000. Attenuated total reflection IR spectroscopy as a tool to investigate the structure, orientation and tertiary structure changes in peptides and membrane proteins. *Biopolymers.* 55:373–380.